

Whole Liver T_1 , T_2 , and T_2^* Relaxation Mapping using Echo Planar Imaging

C. L. Hoad¹, A. G. Gardener¹, J.-Y. Lim¹, C. Costigan², R. C. Spiller³, P. A. Gowland¹, L. Marciani³, G. P. Aithal³, and S. T. Francis¹

¹School of Physics and Astronomy, University of Nottingham, Nottingham, Nottinghamshire, United Kingdom, ²Brain and Body Centre, University of Nottingham, Nottingham, Nottinghamshire, United Kingdom, ³Nottingham Digestive Diseases Centre, NIHR Biomedical Research Unit, University Hospitals NHS Trust, Nottingham, Nottinghamshire, United Kingdom

Introduction: Incidence of chronic liver disease is increasing in the UK with rising prevalence of risk factors such as alcohol excess and obesity in the population. Liver fibrosis, a pathological change in the liver tissue caused by chronic liver injury is currently diagnosed and monitored using liver biopsy, an invasive procedure with associated complications. There have been several recent studies investigating whether MRI and MRS can be used to replace liver biopsy for staging fibrosis [1,2], monitoring iron deposition [3] and estimating liver fat content [4]. Studies have shown that relaxation times (T_1 , T_2 , and T_2^*) can be used to stage cirrhosis (T_1) [5] and determine iron deposition (T_2/T_2^*) [3], however most studies measure only a single relaxation parameter with limited coverage across the liver. The aim of this study was to implement a complete liver relaxation mapping protocol acquiring T_1 , T_2 and T_2^* echo planar images in the same image space. Here we report preliminary measurements of liver tissue relaxation times in chronic liver disease patients and determine whether reproducible histograms of the relaxation maps can be produced from the data which provide a method to discriminate liver tissue from blood vessels.

Methods: The study was approved by the local NHS Ethics Committee and all patients gave written, informed consent. Patients ($n=13$, 9 male) who had chronic liver disease confirmed on liver biopsy were each scanned once on a 1.5 T Philips Achieva scanner with body transmit and a 5-element SENSE cardiac receive coil. All maps were generated from EPI data (9 slices, $3 \times 3 \times 8$ mm voxels, 4 mm slice gap, 96×96 image matrix, SENSE 2, SPIR fat saturation (T_2/T_2^*), water only spectral excitation (T_1)). Data were acquired with respiratory triggering, during the expiration phase of breathing cycle with a minimum TR of 3s (T_2/T_2^*) or 4s (T_1). For T_2 mapping, 3 volumes of SE-EPI data was acquired at each of 6 TEs (27, 35, 42, 50, 60, 70 ms). For T_2^* mapping, 3 volumes of GE-EPI was collected at each of 5 TEs (12, 15, 20, 30, 40 ms). T_1 maps were formed from inversion recovery (IR) SE-EPI data collected at 10 TIs (100-1000 ms). A single inversion pulse was applied per volume (9 slices acquired in 432 ms), the acquisition was performed twice with the slice order reversed (acq1: slices 1-9; acq2: slices 9-1) resulting in all slices being acquired across 20 TIs ranging from 100 to 1484 ms. To ensure that for each TI the slices were acquired during the 'stationary' near-end expiration period, an additional variable delay (T_v) was introduced after the respiratory trigger such that slices were collected at a time $T_v + T_I = 1000$ ms. The total acquisition time of the complete mapping protocol was < 10 mins.

Data Analysis: If respiratory triggering was poor, some through-plane misalignment between slices occurred and these volumes were discarded from the analysis. A mask was drawn around the liver from a single TE/TI volume (9 slices) and each voxel fitted. For the SE-EPI/GE-EPI data, the signal from the voxels within this mask were fitted for T_2/T_2^* using a weighted least squares fit, with $1/TE$ as the weighting factor to generate a 9 slice T_2/T_2^* map. For the IR-EPI sets voxels were fitted to a 3 parameter model for M_0 , T_1 and α (allowing for imperfections in the 180 inversion pulse) using the Powell algorithm. Histogram analysis was used to eliminate the influence of the longer relaxation times of blood in vessels, preventing the need to draw detailed masks to exclude these voxels. To test this hypothesis a Gaussian curve was fitted to the central peak data only (9 bins T_2/T_2^* , 11 bins T_1) and those pixels with non-zero fitted values displayed as overlay maps. Histograms of T_2/T_2^* maps were generated with a bin size of 1 ms and the peak histogram value, FWHM of the peak and the corresponding upper and lower parameter values of this FWHM were then calculated. For the histogram of T_1 data bin sizes of 10 and 20 ms were investigated. To test the reproducibility of histogram analysis a subset of 8 patients were investigated. Three different masks were drawn around each liver on separate occasions and the resulting peak, FWHM and boundary values of the FWHM data were compared. The mean and standard deviation between the 3 maps for each parameter were measured with this standard deviation being quoted as a % of mean.

Results and Discussion: Figure 1 shows an example SE-EPI image and mask, and the generated relaxation maps and the corresponding histograms. The overlay maps are shown for voxels which had a non-zero fit to the Gaussian, and clearly show that most vessels have been excluded from the maps, whilst bulk tissue is included. Figure 2 shows a plot of the histogram mode (peak) T_2 against T_1 , and T_2 against T_2^* for all the liver patients and demonstrates a large spread in these values, with some correlation between T_2 and T_1 and good correlation ($R^2 = 0.9521$) between T_2 and T_2^* . The spread in the data is likely to be a result of differing iron contents and stage of fibrosis. However the study is ongoing and we are currently blinded to the liver biopsy results so cannot currently determine the factors influencing the multi-modal variations in the relaxation times. For the reproducibility study the mask size varied by around 1-2% of its mean size across all subjects and the number of points within the mask not fitting to a positive relaxation parameter was less than 2%. The variation in all the parameters (measured as the mean ($N=8$) percentage standard deviations from the 3 mask measurements) were generally small ($< 1.5\%$) however the bin size as a percentage of the mean peak value measured across all subjects was much larger 2-4%. For the T_2/T_2^* data the histogram bin size was at the minimum value. For the T_1 data the bin size of 20 will be used for future studies as it showed a smaller variation (0.9%) in the FWHM and boundary values of the FWHM parameters than the data with a bin size of 10 (FWHM variation 1.2%) – making all the bin sizes approximately 3-4% of the peak relaxation time measured.

Conclusions: This study has shown it is possible to generate T_2 , T_2^* and T_1 maps covering the whole liver in a reasonable acquisition time. Histogram analysis of the relaxation time maps provided a robust method to separate liver tissue from vessels, with the peak histogram data arising from bulk tissue with minimal vessel contamination and the histogram parameters derived from the data showing minimal dependence on the shape of the mask. Our data shows a spread in measured peak relaxation times in chronic liver disease patients which exceeds the intra-subject variance.

References: [1] Talwalkar J. et al. Hepatology 2008;47:332-342. [2] Kim H. et al. Proc. 16th ISMRM 2008;3715. [3] Wood J. et al. Blood 2005;106:1460-1465.

[4] Longo R. et al. JMRI 1995;5:281-285. [5] Keevil S. et al. Brit. J. Radiol. 1994;67:1083-1087

Acknowledgements: This work was funded by a Strategic Funding Initiative from the Biomedical Research Committee at the University of Nottingham.

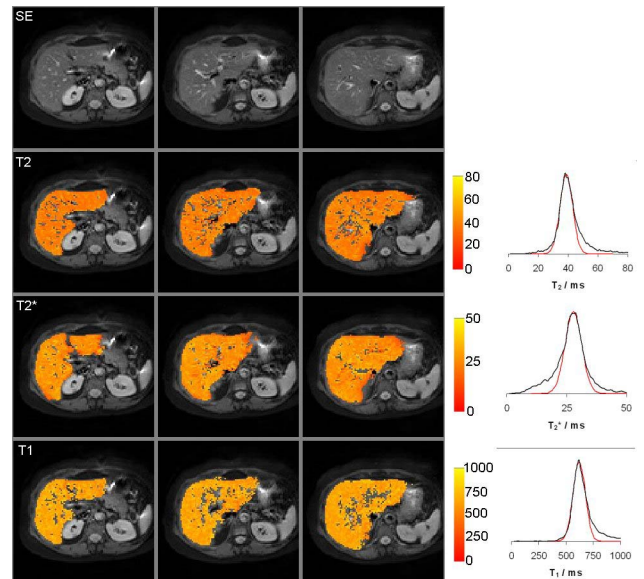


Figure 1. Base SE liver images from a liver patient with T_2 , T_2^* and T_1 maps overlaid (3 slices of 9 slice data set shown). Corresponding histograms (black curve) from the 9 slice data set, and the Gaussian curve fitted to the central peak only (red curve). Colour overlay displays only pixel values where the red curve is non-zero

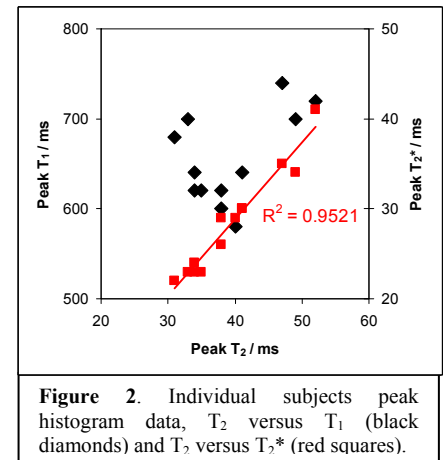


Figure 2. Individual subjects peak histogram data, T_2 versus T_1 (black diamonds) and T_2 versus T_2^* (red squares).